Novel Molecular Signaling and Classification of Human Clinically Nonfunctional Pituitary Adenomas Identified by Gene Expression Profiling and Proteomic Analyses

Carlos S. Moreno,[1] Chheng-Orn Evans,[2] Xianquan Zhan,[3] Mammerhi Okor,[6] Dominic M. Desiderio,[3,4,5] and Nelson M. Oyesiku[2]

[1]Department of Pathology and Laboratory Medicine and Winship Cancer Institute and [2]Department of Neurosurgery and Laboratory of Molecular Neurosurgery and Biotechnology, Emory University School of Medicine, Atlanta, Georgia; [3]Charles B. Stout Neuroscience Mass Spectrometry Laboratory and Departments of [4]Neurology and [5]Molecular Sciences, University of Tennessee, Health Science Center, and University of Tennessee Cancer Institute, Tennessee; and [6]Department of Neurosurgery, University of Alabama School of Medicine, Birmingham, Alabama

Abstract

Pituitary adenomas comprise 10% of intracranial tumors and occur in about 20% of the population. They cause significant morbidity by compression of regional structures or the inappropriate expression of pituitary hormones. Their molecular pathogenesis is unclear, and the current classification of clinically nonfunctional tumors does not reflect any molecular distinctions between the subtypes. To further elucidate the molecular changes that contribute to the development of these tumors and reclassify them according to the molecular basis, we investigated 11 nonfunctional pituitary adenomas and eight normal pituitary glands, using 33 oligonucleotide GeneChip microarrays. We validated microarray results with the reverse transcription real-time quantitative PCR, using a larger number of nonfunctional adenomas. We also used proteomic analysis to examine protein expression in these nonfunctional adenomas. Microarray analysis identified significant increases in the expression of 115 genes and decreases in 169 genes, whereas proteomic analysis identified 21 up-regulated and 29 down-regulated proteins. We observed changes in expression of SFRP1, TLE2, PITX2, NOTCH3, and DLK1, suggesting that the developmental Wnt and Notch pathways are activated and important for the progression of nonfunctional pituitary adenomas. We further analyzed gene expression profiles of all nonfunctional pituitary subtypes to each other and identified genes that were affected uniquely in each subtype. These results show distinct gene and protein expression patterns in adenomas, provide new insight into the pathogenesis and molecular classification of nonfunctional pituitary adenomas, and suggest that therapeutic targeting of the Notch pathway could be effective for these tumors. (Cancer Res 2005; 65(22): 10214-22)

Introduction

Pituitary adenomas account for ~10% of intracranial tumors and occur in about 20% of the population. They cause significant morbidity by compression of regional structures and the inappropriate expression of pituitary hormones (1, 2). Nonfunctional pituitary adenomas, so-called because they do not cause clinical hormone hypersecretion (2–5), account for ~30% of pituitary tumors (3). The nonfunctional tumors are uniquely heterogeneous (Table 1), typically quite large, and cause hypopituitarism or blindness from regional compression (1).

Despite the lack of clinical hormone hypersecretion, immunocytochemical staining for hormones reveals evidence for hormone expression in up to 79% of these tumors, which we will refer to as immunohistochemically positive nonfunctional (NF^+) tumors. The remainder are negative for hormone expression (2, 5) and will be referred to as immunohistochemically negative nonfunctional (NF^-) tumors. However, current pathologic classification (Table 1) of these tumors has no molecular basis, and surprisingly, is based only on anterior pituitary hormone histochemistry for hormones, or on electron microscopy, which is of limited use.

Unlike the functional pituitary tumors, there is no available effective medical therapy for the nonfunctional tumors, and only a better understanding of the molecular biology of these tumors will provide needed medical treatment options.

Although pituitary tumors are mostly benign, 5% to 35% of them are locally invasive. A small number exhibit a more aggressive course, infiltrate dura, bone and sinuses and are highly aggressive. A significantly smaller number are truly malignant; that is, they metastasize outside the central nervous system. It is not known what molecular profiles result in local invasion or presage a more aggressive course.

Molecular genetic studies have shown that these tumors are monoclonal in origin (6, 7). A minority is part of an autosomal-dominant syndrome, multiple endocrine neoplasia type 1 (MEN1), which is associated with mutations in the *MEN1* tumor suppressor gene. Others are associated with loss of heterozygosity on the 11q13 chromosome (2, 8–10). A dominant mutation occurs in the *Gαs* gene in ~30% of somatotrophinomas, but this mutation is rare in other pituitary tumors (2, 11, 12). In nonfunctional tumors, reduced levels of expression of the retinoid X receptor, estrogen receptor, and thyroid hormone receptor have been found and may contribute to abnormal thyroid hormone regulation of α-subunit production in these tumors. However, the significance of these data to pituitary tumorigenesis is unknown (13). The epidermal growth factor receptor (EGFR) is overexpressed in 80% of nonfunctional adenomas and is virtually undetectable in functional adenomas. *In vitro*, nonfunctional tumors in culture proliferate in response to EGF administration and up-regulate EGFR mRNA (14). In addition, we

Note: Supplementary data for this article are available at Cancer Research Online (http://cancerres.aacrjournals.org/).

The laboratory of D.M. Desiderio contributed the proteomic data, and the laboratory of N.M. Oyesiku contributed the microarray and reverse transcriptase real-time quantitative PCR data to this study.

Requests for reprints: Nelson M. Oyesiku, Department of Neurosurgery, Emory University School of Medicine, 1365-B Clifton Road Northeast, Suite 6400, Atlanta, GA 30322. Phone: 404-778-4737; Fax: 404-778-4472; E-mail: noyesik@emory.edu.

doi:10.1158/0008-5472.CAN-05-0884

Table 1. Classification of nonfunctional pituitary adenomas by cell of origin

Cell type	Hormone expression	% Nonfunctional tumors
Null cell	None	17
Oncocytoma	None	6
Silent corticotroph	ACTH	8
Silent somatotroph	GH	3
Gonadotrophs	Intact LH/FSH or subunits	40-79

recently found that the folate receptor is overexpressed in nonfunctional pituitary adenomas (15, 16).

To further elucidate the molecular changes that contribute to the development of these tumors and reclassify them according to the molecular basis, we used microarray analysis to elucidate the gene expression profile of 11 nonfunctional pituitary adenomas compared with eight normal pituitary glands.

We verified the gene expression changes of four genes that were detected by microarray analysis in 23 nonfunctional pituitary tumors and eight normal pituitary glands by reverse transcription real-time quantitative PCR (RT-qPCR). To complement and extend the expression profiling data, a comparative proteomics system based upon two-dimensional PAGE and mass spectrometry (MS) were used to characterize each differentially expressed protein in the same pituitary adenoma tissues.

Materials and Methods

Patients and tumor characterization. Sporadic pituitary adenomas were obtained from patients at the Emory University Hospital during transsphenoidal surgery (Supplementary Table 1). Informed consent for inclusion in this study was obtained. Pituitary adenomas are anatomically and pathologically distinct from the normal anterior lobe, making them easy to dissect under the surgical microscope. All tumors were microdissected and removed using the surgical microscope, rinsed in sterile saline, snap-frozen in liquid nitrogen, and stored (−80°C) for molecular analysis and proteomics. Each tumor fragment was then confirmed independently by a neuropathologist as being homogenous and unadulterated by histology and immunohistochemistry before molecular analysis.

Eight normal pituitary glands obtained from the National Hormone and Pituitary Program, National Institute of Diabetes and Digestive and Kidney Diseases (Bethesda, MD; $n = 3$) and from the National Disease Research Interchange (Philadelphia, PA; $n = 5$) were used as controls for microarray and RT-qPCR analyses. Eight normal pituitary glands obtained from the Memphis Regional Medical Center ($n = 7$) and the National Disease Research Interchange ($n = 1$) were used as controls in proteomics.

Synthesis of biotin-labeled cRNA and microarray hybridization. Total RNA extraction was previously described (15, 16). Briefly, total RNA (100 μg) was purified, using the RNeasy Mini Kit (Qiagen, Inc., Valencia, CA) with minor modifications. Total RNA was eluted twice with 50 μL of 65°C DEPC-treated water. Double-strand cDNA was synthesized from 25 μg total RNA with the Superscript II (Invitrogen, Carlsbad, CA) and a T7-(dT) 24 oligomer then purified by phase-lock gel (Eppendof, Wesbury, NY) with phenol/chloroform extraction. Biotin-labeled cRNA was produced with Enzo BioArray High Yield RNA Transcription Labeling kit according to the manufacturer's instructions. The biotinylated cRNA was fragmented to 50 to 200 nucleotides by heating (94°C for 35 minutes) and chilled on ice.

For microarray analysis, three normal pituitary glands and 11 nonfunctional pituitary adenomas were analyzed using HG-U95Av2 GeneChips (Affymetrix, Santa Clara, CA) at the Emory/Veterans' Administration Medical Center (Atlanta, GA). All samples were analyzed in duplicate, starting from the extraction of total RNA, GeneChip hybridization, washing, scanning, and data analysis. Five additional normal pituitary glands were analyzed once using the same chips, HG-U95Av2 GeneChips at the Moffit Comprehensive Cancer Center, University of South Florida (Tampa, FL).

Data analysis. Gene expression data from 12,625 probe sets on the HG-U95Av2 GeneChips were normalized, using GCRMA normalization with GeneTraffic Software (Iobion, La Jolla, CA). After data normalization, genes with uniformly low expression were removed from consideration, leaving 7,241 probe sets for analysis using significance analysis of microarrays (SAM) software (17). The following are the relevant variables for the SAM analysis: imputation engine, 10-nearest neighbor; number of permutations, 500; RNG seed, 1234567; delta, 1.063; fold change, 2.0. Normalized expression data from the 297 significant probe sets were analyzed by a two-dimensional hierarchical clustering, using Spotfire DecisionSite 8.1 software. Data was clustered using unweighed averages and ordered using average Euclidian distance.

For K-nearest neighbor (KNN) prediction, the normalized RT-qPCR data was analyzed with GenePattern software (http://www.broad.mit.edu/cancer/software/genepattern/), and both the KNN cross-validation and class prediction modules were used (KNN = 3). For these analyses, the four genes (or features) that were included were NADP-dependent isocitrate dehydrogenase (*IDH1*), paired-like homeodomain transcription factor 2 (*PITX2*), Notch homologue 3 (*NOTCH3*), and delta-like 1 homologue (*Drosophila*, *DLK1*).

To identify genes uniquely altered in tumor subtypes, SAM analysis was done with both the normal samples and other tumor subtypes as the control group, and the subtype of interest as the experimental group. Analyses were done with 500 permutations, fold change of 2.0, and false discovery rate (FDR) < 1%.

Reverse transcriptase real-time quantitative PCR. RT-qPCR was done as described (15, 16) on four gene transcripts in 23 nonfunctional pituitary adenomas and eight normal pituitary glands in a blinded fashion. Primers were selected using Primer Express software, version 2.0 (PE Applied Biosytems, Foster City, CA), BLASTed against all *Homo sapiens* gene sequences in Genbank for selectivity. The following are the primers of these genes:

	Forward primer	Reverse primer
IDH1	CACTACCGCATGT ACCAGAAAGG	TCTGGTCCAGGC AAAAATGG
PITX2	GCCGGGATCGTAG GACCTT	GTGCCCACGACC TTCTAGCA
NOTCH3	TCTCAGACTGGTC CGAATCCAC	CCAAGATCTAAGA ACTGACGAGCG
DLK1	CACATGCTGCGGA AGAAGAAGAAC	ACCGCGTATAGTAA GCTCTGAGGA

rRNA (18S rRNA from PE Applied Biosystems) was used as an internal control. All PCR reactions were done at least in duplicate and cycled in the GeneAmp 5700 Sequence Detection System: 50.0°C for 2 minutes, 95.0°C for 10 minutes, and 40 cycles of 95.0°C for 15 seconds and 60.0°C for 1 minute. The quantity of the specific genes obtained from standard curves was normalized to that of the 18S rRNA of the same sample. Fold change of each gene was calculated as the ratio of the mean of the normalized mRNA of nonfunctional compared with that of the normal pituitary controls.

Two-dimensional gel electrophoresis of pituitary proteins. The detailed experimental protocols have been published (18, 19). Briefly, each whole control pituitary tissue (0.45-0.70 g; $n = 8$) and each adenoma tissue (15-75 mg; $n = 11$) was homogenized and lyophilized, and the protein content was measured. For an 18-cm IPG strip, pH 3 to 10 nonlinear (Amersham Pharmacia Biotech, Piscataway, NJ), a total of 70 μg of pituitary protein was used for two-dimensional gel electrophoresis. Isoelectric focusing was done on a Multiphor II instrument (Amersham Pharmacia Biotech) with precast IPG strips (pH 3-10, nonlinear, 180 × 3 × 0.5 mm). SDS-PAGE was done on a PROTEAN plus Dodeca Cell (Bio-Rad, Hercules, CA) that can analyze up to 12 gels at a time with a 12% PAGE resolving gel (190 × 205 × 1.0 mm) that was

cast with a PROTEAN plus Multicasting Chamber (Bio-Rad). The two-dimensional gel electrophoresis–separated proteins were visualized with a modified silver-staining method. The differential spots were determined between control pituitaries (n = 8, number of gels = 30) versus NF^- (n = 2, number of gels = 6), LH^+ (n = 3, number of gels = 9), FSH^+ (n = 3, number of gels = 9), FSH^+ and LH^+ (n = 3, number of gels = 9).

Image analysis of digitized two-dimensional gels. The silver-stained two-dimensional gels were digitized, and the digitized gels were analyzed qualitatively and quantitatively with the PDQuest two-dimensional Gel Analysis software for a PC computer (version 7.1.0, Bio-Rad). The total density in a gel image was used to normalize each spot volume in the gel image to minimize the effect of any experimental factor on the quantitative analysis (19–21). Gel images in the match set were grouped into the following: control, NF^-, LH^+, FSH^+, and FSH^+ and LH^+. The comparison analyses were done with the average normalized-volume among the five groups.

Mass spectrometry characterization of proteins. Each differential spot was labeled, excised from the two-dimensional gels, and subjected to in-gel trypsin digestion (18). That mixture of tryptic peptides was purified with a ZipTipC18 microcolumn (ZTC18S096, Millipore, Bedford, MA) according to the manufacturer's instructions. The purified tryptic-peptide mixture was analyzed with a Perseptive Biosystems matrix-assisted laser desorption/ionization time-of-flight (MALDI-TOF) Voyager DE-RP mass spectrometer (Framingham, MA) and with an LCQ^{Deca} mass spectrometer (LC-ESI-Q-IT) equipped with a standard electrospray source

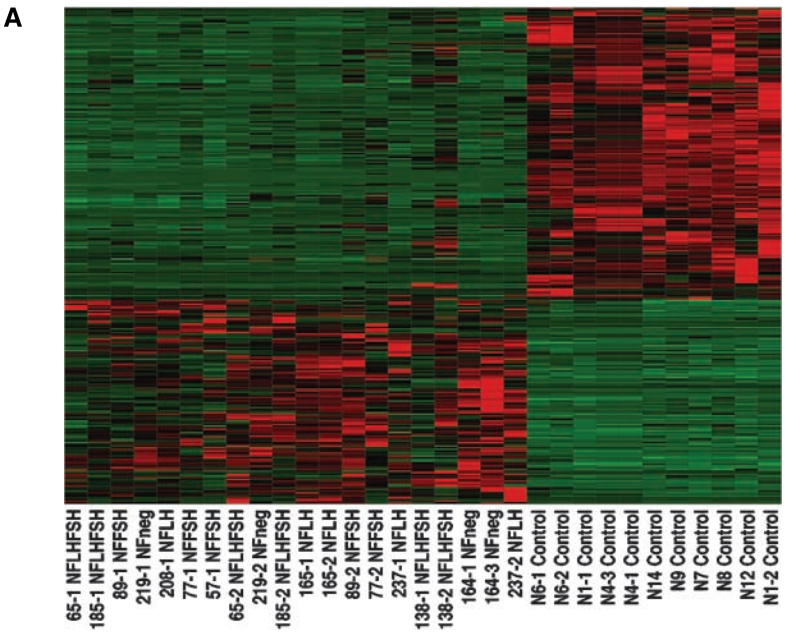

C

RT-qPCR K-nearest neighbor Predictions (KNN = 3, Genes = 4)

Leave-One-Out Cross Validation

	True Normal	True Tumor	Errors
Normal Pred	8	0	0
Tumor Pred	0	23	0

Independent Training and Test Sets

Train Set (n = 21)

	True Normal	True Tumor
	5	16

Test Set (n = 10)

	True Normal	True Tumor	Errors
Normal Pred	3	0	0
Tumor Pred	0	7	0

Figure 1. *A,* expression pattern of genes that are significantly different between nonfunctional pituitary adenomas and normal pituitary tissues analyzed by two-dimensional hierarchical clustering. *Red,* higher expression; *green,* lower expression; *black,* nonsignificant genes. *B,* RT-qPCR of relative expression of IDH1, PITX2, NOTCH3, and DLK1 mRNAs in nonfunctional adenomas (n = 23) compared with normal pituitaries (n = 8). *Columns,* mean mRNA expression of each gene in nonfunctional tumors or normal pituitary glands; *bars,* SE. Increased expression for IDH1 (41-fold), PITX2 (14-fold), and NOTCH3 (14-fold) were all confirmed by RT-qPCR. Decreased expression for DLK1 was also confirmed (−717-fold). *C,* prediction results of KNN analysis using RT-qPCR data for IDH1, PITX2, NOTCH3, and DLK1. Predictions generated with GenePattern software were 100% correct with both leave-one-out cross-validation and with independent training and test sets.

Table 2. Expression changes of selected genes in nonfunctional adenomas

Probe set ID	Symbol	Gene name	Gene Ontology category	Fold change
39930_at	*EPHB6*	EphB6	Signal transduction	15.09
203_at	*GATA2*	GATA binding protein 2	Transcription	14.55
35243_at	*PCTK3*	PCTAIRE protein kinase 3	Cell cycle	14.07
39023_at	*IDH1*	Isocitrate dehydrogenase 1 (NADP+), soluble	Metabolism	13.10
40511_at	*GATA3*	GATA binding protein 3	Transcription	12.76
41014_s_at	*PITX2*	Paired-like homeodomain transcription factor 2	Transcription	12.44
821_s_at	*FOLR1*	Folate receptor 1 (adult)	Transport	5.66
424_s_at	*FGFR1*	Fibroblast growth factor receptor 1	Signal transduction	4.27
38750_at	*NOTCH3*	Notch homologue 3	Transcription	4.26
2054_g_at	*CDH2*	N-cadherin	Cell adhesion	3.23
32565_at	*SMARCD3*	SWI/SNF related d3	Transcription	3.00
37920_at	*PITX1*	Paired-like homeodomain transcription factor 1	Transcription	2.92
469_at	*EFNB3*	Ephrin-B3	Cell-cell signaling	2.42
871_s_at	*HLF*	Hepatic leukemia factor	Transcription	2.34
41715_at	*PIK3C2B*	Phosphoinositide-3-kinase, class 2, beta	Signal transduction	2.26
823_at	*CX3CL1*	Chemokine (C-X3-C motif) ligand 1	Cell motility	2.24
40837_at	*TLE2*	Transducin-like enhancer of split 2	Development	2.03
33596_at	*SPOCK3*	Testican 3	Integral membrane	2.01
41536_at	*ID4*	Inhibitor of DNA binding 4	Transcription	−2.18
33904_at	*CLDN3*	Claudin 3	Cell adhesion	−2.47
1586_at	*IGFBP3*	Insulin-like growth factor binding protein 3	Apoptosis	−2.59
1909_at	*BCL2*	B-cell CLL/lymphoma 2	Apoptosis	−2.71
41839_at	*GAS1*	Growth arrest–specific 1	Cell cycle	−3.62
38010_at	*BNIP3*	BCL2/adenovirus E1B 19-kDa interacting protein 3	Apoptosis	−3.85
37043_at	*ID3*	Inhibitor of DNA binding 3	Transcription	−4.10
36199_at	*DAP*	Death-associated protein	Apoptosis	−4.56
40570_at	*FOXO1A*	Forkhead box O1A (rhabdomyosarcoma)	Transcription	−5.79
37005_at	*NBL1*	Neuroblastoma, suppression of tumorigenicity 1	Oncogenesis	−6.08
32786_at	*JUNB*	jun B proto-oncogene	Transcription	−6.12
39822_s_at	*GADD45B*	Growth arrest and DNA damage–inducible, β	Signal transduction	−6.24
41215_s_at	*ID2*	Inhibitor of DNA binding 2	Transcription	−6.30
39352_at	*CGA*	Glycoprotein hormones, α polypeptide	Cell-cell signaling	−7.53
31874_at	*GAS2L1*	Growth arrest–specific 2 like 1	Cell cycle	−9.04
36617_at	*ID1*	Inhibitor of DNA binding 1	Transcription	−9.73
35378_at	*LHB*	LH β polypeptide	Hormone	−12.96
1916_s_at	*FOS*	v-fos osteosarcoma viral oncogene homologue	Transcription	−15.90
649_s_at	*CXCR4*	Chemokine (C-X-C motif) receptor 4	Cell motility	−16.36
36784_at	*CSHL1*	Chorionic somatomammotropin hormone-like 1	Hormone	−85.03
878_s_at	*PRL*	Prolactin	Hormone	−100.81
40544_g_at	*ASCL1*	Achaete-scute complex-like 1 (*Drosophila*)	Neurogenesis	−116.82
40316_at	*GH2*	Growth hormone 2	Hormone	−307.69
309_f_at	*GH2*	Growth hormone 2	Hormone	−578.03
32648_at	*DLK1*	Delta-like 1 homologue (*Drosophila*)	Development	−917.43
1332_f_at	*GH1*	Growth hormone 1	Hormone	−5,000.00

(ThermoFinnigan, San Jose, CA). For MALDI-TOF MS analysis, the peptide-mass fingerprinting (PMF) data were generated. For liquid chromatography electrospray ionization ion-quadrupole-ion trap (LC-ESI-Q-IT) analysis, the amino acid sequence of each LC-separated tryptic peptide was obtained. The MALDI-TOF MS PMF data were used to identify the protein by searching the SWISS-PROT/TrEMBL database with PeptIdent software (http://us.expasy.org/tools/peptident.html). The LC-ESI-Q-IT tandem MS (MS/MS) data were used to identify the protein by searching the SWISS-PROT and NCBInr databases with the SEQUEST software that is a part of the LCQ^{Deca} software package.

Results

The clinical and pathologic characteristics of all nonfunctional pituitary tumors in this study are summarized in Supplementary Table 1. The 11 pituitary tumors used in microarray analysis included tumors immunohistochemically negative for anterior pituitary hormones (NF^-, $n = 2$), positive for luteinizing hormone (LH^+, $n = 3$), positive for follicle-stimulating hormone (FSH^+, $n = 3$), and positive for both FSH and LH (FSH^+ and LH^+, $n = 3$). These same 11 tumors were used in proteomic and RT-qPCR analyses. A total of 23 nonfunctional tumors were used for RT-PCR analysis (Supplementary Table 1).

Cluster analysis of gene expression by microarray analysis. Data from two replicate hybridizations (57-2 and 208-2) were of poor quality and removed from the analysis. To identify genes that were differentially expressed between tumor and normal pituitary samples in a statistically significant manner, we used the SAM software (17). Using a highly conservative threshold (fold change

> 2.0, FDR < 1%), we identified 297 probe sets corresponding to 284 unique genes that were significantly different between pituitary tumors and normal tissues. Normalized expression data from these 297 probe sets were analyzed by two-dimensional hierarchical clustering (Fig. 1*A*). A complete list of these 284 unique genes is given in Supplementary Table 2, and a subset of those genes is provided in Table 2. In general, tumor suppressors (e.g., *NBL1*) and apoptosis inducers (*BNIP3*) were down-regulated, whereas antiapoptotic genes (*PIK3C2B* and *FAIM2*) were up-regulated. In addition, the apoptosis inhibitor BCL2 was down-regulated by >3-fold compared with normal pituitary, suggesting that other antiapoptotic mechanisms are at work in nonfunctional pituitary adenomas. Positive regulators of cell cycle progression, such as PCTAIRE protein kinase 3, exhibited an increased expression, whereas negative cell cycle regulators, such as GADD45β and GAS1, were down-regulated.

Two components of the delta-Notch pathway, NOTCH3 and DLK1, were strongly altered in opposite directions. NOTCH3 was up-regulated nearly 5-fold, whereas DLK1 was repressed over 900-fold. In addition, human achaete-scute homologue (ASCL1/HASH1), which is essential for DLK1 expression, was down-regulated over 100-fold. The fibroblast growth factor receptor 1 (FGFR1) was up-regulated over 3-fold in nonfunctional pituitary adenomas. In addition, expression of the insulin-like growth factor binding protein 3 (IGFBP3), which decreases IGF availability and signaling, was reduced 3-fold compared with normal tissues.

Over 50 transcription factors were altered in their expression in nonfunctional pituitary adenomas, making it one of the largest functional categories (Supplementary Table 2). Several developmental transcription factors, including NOTCH3, PITX1, PITX2, and PBX3, were up-regulated, whereas others, such as C/EBPδ, were down-regulated. Surprisingly, the inhibitors of the DNA-binding family (ID1, ID2, ID3, and ID4), which are inhibitors of neural differentiation and are frequently overexpressed in neuroectodermal tumors (22), were all down-regulated in pituitary adenomas. Some transcription factors associated with oncogenesis, such as FOS, JUNB, and FOXO1A/FKHR, were also down-regulated. Nevertheless, decreased levels of FOXO1A/FKHR are consistent with an elevated signaling through the phosphatidylinositol 3-kinase/PTEN/AKT pathway, because AKT activation results in the exclusion of FKHR from the nucleus (23).

Several genes that enhance cell motility and invasion were increased in nonfunctional pituitary adenomas, including *ephrin receptor B6, ephrin B3, testican 3, N-cadherin 2*, and the chemokine ligand *CX3CL1*. The down-regulation of the tight-junction molecule claudin 3 was consistent with a cellular phenotype of increased motility. Moreover, our gene expression profiling results were consistent with the expectations for the nonfunctional tumors. For example, the up-regulation of the folate receptor (FOLR1) was consistent with our previous observations (15, 16). In addition, LH, growth hormone 1, growth hormone 2, chorionic somatomammotropin hormone-like 1, and prolactin were all strongly down-regulated as expected.

Validation of expression array result by reverse transcription real-time quantitative PCR analysis. To validate the microarray analysis, we measured with RT-qPCR, using SYBR Green I dye detection the mRNA expression levels of IDH1, PITX2, NOTCH3, and DLK1 using blinded samples which consisted of 23 nonfunctional tumors and eight normal pituitary glands. The 23 nonfunctional tumors composed of six FSH^+, six LH^+, six FSH^+ and LH^+, and five NF^- (Supplementary Table 1). Using blinded samples

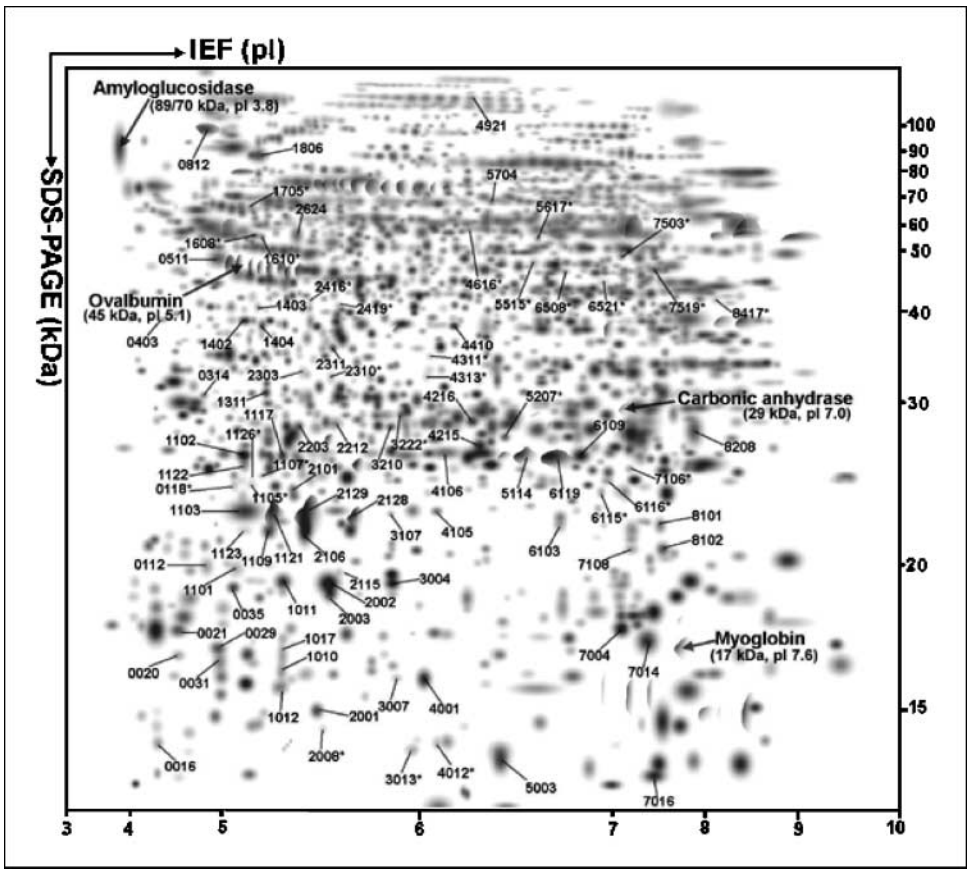

Figure 2. A digitized two-dimensional gel electrophoresis reference map (Gaussian image) from a human control pituitary proteome labeled with the 93 differential spots and the four protein standard markers. Isoelectric focusing (*IEF*) was done with an 18-cm IPG strip (pH 3-10, nonlinear), and vertical SDS-PAGE was done with a 12% polyacrylamide gel.

Table 3. Molecular classification of nonfunctional tumors by subtype by gene expression profile analysis

Subtype	Fold change	Gene symbol	Probe set ID	Accession no.	Title
FSH^+	4.7	*CXCL13*	41104_at	NM_006419	Chemokine (C-X-C motif) ligand 13
FSH^+	2.7	*HPIP*	38063_at	NM_020524	Hematopoietic PBX-interacting protein
FSH^+	2.2	*KRT19*	40899_at	NM_002276	Keratin 19
LH^+	4.5	*MLP*	36174_at	NM_023009	MARCKS-like protein
LH^+	2.7	*GUCY1A3*	36918_at	NM_000856	Guanylate cyclase 1, soluble, α 3
LH^+	2.4	*TMPRSS6*	34067_at	NM_153019	Type II transmembrane serine protease 6
LH^+	2.4	*BASP1*	32607_at	NM_006317	Brain abundant, membrane attached signal protein 1
NF^-	15.9	*C7*	37394_at	NM_000587	Complement component 7
NF^-	5.9	*PDLIM1*	36937_s_at	NM_020992	PDZ and LIM domain 1 (elfin)
NF^-	4.6	*HIST1H2AC*	34308_at	NM_003512	Histone 1, H2ac
NF^-	4.1	*GPR49*	41073_at	NM_003667	G protein–coupled receptor 49
NF^-	3.9	*SYT1*	40075_at	NM_005639	Synaptotagmin I
NF^-	3.7	*ALS2CR3*	40064_at	NM_015049	Amyotrophic lateral sclerosis 2, candidate 3
NF^-	3.6	*HIST1H2BL*	35576_f_at	NM_003519	Histone 1, H2bl
NF^-	3.3	*HIST2H2AA*	286_at	NM_003516	Histone 2, H2aa
NF^-	3.1	*HIST1H2BN*	36347_f_at	NM_003520	Histone 1, H2bn
NF^-	3.0	*PTPN3*	31885_at	NM_002829	Protein tyrosine phosphatase, nonreceptor type 3
NF^-	2.3	—	34114_at	AL109678	cDNA clone EUROIMAGE 28993.
NF^-	2.2	*HIST1H2BM*	31528_f_at	NM_003521	Histone 1, H2bm
NF^-	2.2	*HIST1H2BK*	32819_at	NM_080593	Histone 1, H2bk
NF^-	2.2	*AGPAT1*	32836_at	NM_006411	1-Acylglycerol-3-phosphate *O*-acyltransferase 1

NOTE: Genes that were altered specifically in each subtype of nonfunctional adenomas are shown. NF^-, negative immunohistochemical stains for ACTH, LH, FSH, PRL, GH, and TSH.
Adenomas were graded blindly by a neuropathologist from 0 to 4 for intensity of staining for each peptide hormone.

to do RT-qPCR, the normalized value of each gene of each sample was used to classify the sample in two groups (nonfunctional and control groups) correctly. RT-qPCR analysis showed that IDH1, PITX2, and NOTCH3 mRNAs were significantly up-regulated respectively 41-fold, 14-fold, and 14-fold in nonfunctional pituitary adenomas, and that DLK1 mRNA expression was down-regulated 717-fold (Fig. 1*B*).

We next used the RT-qPCR data to attempt to classify the nonfunctional tumor and normal samples using the KNN method. With the GenePattern software (http://www.broad.mit.edu/cancer/software/genepattern/), the tumor and normal samples were correctly predicted in 100% of the cases using the normalized RT-qPCR data for these four genes (Fig. 1*C*). This level of accuracy was achieved both with leave-one-out cross-validation and when the data was separated into independent training sets (n = 21) and test sets (n = 10).

Proteomic analysis of human nonfunctional pituitary adenoma and control samples. The proteomes from control pituitary versus NF^-, LH^+, FSH^+, and FSH^+ and LH^+ tumors were analyzed by two-dimensional gel electrophoresis. Each sample was analyzed three to five times, and ca. 1,000 protein spots were detected in each gel (Fig. 2 contains a digital master gel map). For each sample, the correlation coefficient (r) of the normalized volumes between-gel matched spots was >0.73 (range, 0.76-0.92), and the mean between-gel, matched percentage was 85% to 99% for the controls and 81% to 90 % for the adenomas. A total of 93 differential protein spots were found among the different cell types of nonfunctional adenomas. Each differential spot was labeled in the digital master gel map (Fig. 2). Supplementary Table 3 contains those MS-characterized protein spots for which the spot volume in the control group was significantly different from each adenoma group ($P < 0.001$). Differential spots were excised, in-gel trypsin digestion was done, and MS (MALDI-TOF PMF and/or LC-ESI-Q-IT MS/MS) was used to characterize the protein in each differential spot (18). Among those 93 differential spots, 72 spots contained 50 differentially regulated proteins (21 up-regulated and 29 down-regulated) that were characterized. MS/MS data were used to search the database with SEQUEST software.

The 50 MS-characterized differentially expressed proteins were categorized into several different functional groups (Supplementary Table 3). Identified proteins that were affected in nonfunctional adenomas included the following: (a) Neuroendocrine-related proteins, including somatotropin, secretagogin, and mu-crystallin homologue, were down-regulated in the nonfunctional pituitary adenomas. (b) At least 17 isoforms of somatotropin were down-regulated. (c) Immunologic regulation proteins and tumor-related antigen (immunoglobulin, tumor rejection antigen 1) were down-regulated. (d) Cell proliferation, differentiation, and apoptosis-related proteins were down-regulated. (e) Cell defense and stress resistance proteins (phospholipid hydroperoxide glutathione peroxidase, CD59 glycoprotein, and heat shock 27-kDa protein) were down-regulated. (f) Some metabolic enzyme-related proteins (IDH [NADP] cytoplasmic, tryptophan 5-hydroxylase 2, matrix metalloproteinase-9, aldose reductase, lactoylglutathione lyase, acyl-CoA-binding protein) were up-regulated in the nonfunctional pituitary adenomas.

Proteomic validation of gene expression profiling data. We compared the proteomic data with gene expression profiling data for consistency at the protein and the mRNA levels. Whereas expression profiling identified 284 altered genes, proteomics

identified 50 altered proteins (10.7%). Of these 50 proteins, only 40 had corresponding probe sets present on the U95A GeneChip. Of those 40 detectable genes, 31 genes (77.5%) were detected as present at the mRNA level. Four of these genes (*IDH1, GH1, GH2*, and *PRL*) met our mRNA significance criteria and were identified by both experimental approaches. Thirteen additional genes (32.5%) did not meet our significance criteria but nevertheless had mRNA changes of >1.3-fold in the same direction as observed changes at the protein level. Only one gene (*Thioredoxin domain containing 9*, O14530) had opposite changes and was decreased at the protein level but increased (1.32-fold) at the mRNA level. Finally, 32.5% of the altered proteins showed essentially no change at the mRNA level. In general, there was quite good agreement between the proteomics and expression data (43%), although not surprisingly, there were proteins with altered abundance that showed little if any change at the level of transcription. These genes are likely regulated by altered translational efficiencies and posttranslational effects on protein stabilities.

Molecular classification of nonfunctional pituitary tumors by subtype. We further analyzed the gene expression profiles of all four nonfunctional pituitary subtypes to each other and identified genes that were affected uniquely in each subtype (Table 3). To qualify for this description, the genes had to be significantly different in only a single subtype relative to normal tissue and also be significantly different between that tumor subtype and the other tumor subtypes. No genes were uniquely altered in the nonfunctional tumors that expressed both the LH^+ and FSH^+ subtype. In the nonfunctional tumors that expressed FSH^+ subtype, *CXCL13* and hematopoietic PBX-interacting protein were up-regulated. In the nonfunctional tumors that expressed LH^+ subtype, uniquely up-regulated genes included *MLP, GUCY1A3, TMPRSS6*, and *BASP1*. In the NF^- subtype tumors, 14 genes were uniquely up-regulated, including four Histone 2b variants, two Histone 2a variants, and *synaptotagmin I*.

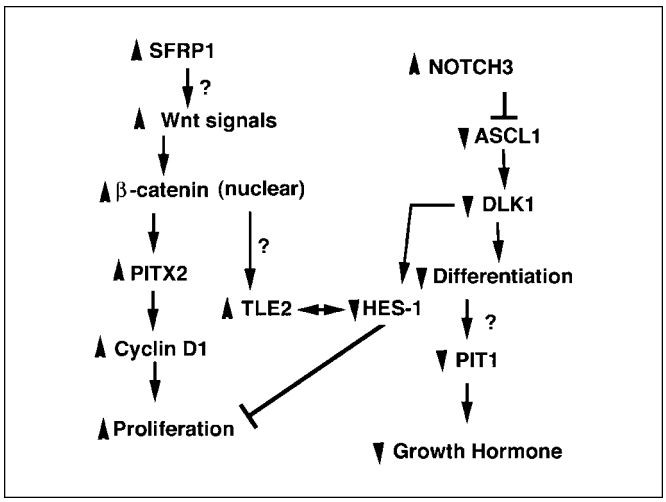

Figure 3. A model of the effects of Wnt and Notch signaling on nonfunctional pituitary adenomas. Genes with an increased mRNA level (*up arrow*) and with a decreased expression (*down arrow*). In this model, increased SFRP1 activates the Wnt pathway, resulting in nuclear β-catenin, increased PITX2, elevated cyclin D1, and cellular proliferation. In parallel, increased NOTCH3 represses HASH1/ASCL1, resulting in reduced DLK1 and inhibiting cellular differentiation, and PIT1 and GH expression. How increased TLE2 and decreased HES-1 levels affect tumor progression requires further investigation but may enhance proliferation and inhibit differentiation.

Discussion

Our gene expression profiling of nonfunctional pituitary adenomas identified 115 up-regulated genes and 169 down-regulated genes. Some gene profiles showed good agreement with the proteomic data. In addition, the gene expression data were consistent with expected results for a number of genes, such as *FOLR1, growth hormone*, and prolactin *Pit-1*. The RT-qPCR results of all four genes tested (*IDH1, PITX2, NOTCH3*, and *DLK1*) confirmed our gene expression profiling data.

We observed increased levels of IDH1 mRNA by gene expression profiling, RT-qPCR, and proteomic analysis. IDHs (24) catalyze oxidative decarboxylation of isocitrate into α-ketoglutarate. In addition, mitochondrial and cytosolic NADP(+)-dependent IDHs play an important role in cellular defense against oxidative damage as a source of NADPH (25, 26). Moreover, NADP-dependent IDH is up-regulated in human colon tumors (27) and may prevent apoptosis in tumors cells via detoxification of tumor therapeutic drugs (28).

Our observation that PITX2 is overexpressed in nonfunctional pituitary adenomas is consistent with previous analyses of human pituitary adenomas (29). *PITX1* (also known as *P-OTX*) and *PITX2* specify closely related bicoid transcription factors that appear early, are made in multiple tissues, and continue to be expressed in adult life (30, 31). *PITX2*a and *PITX1* both interact with *Pit-1*, a master regulator of pituitary cell differentiation, thyroid-stimulating hormone, growth hormone, and prolactin genes (31, 32).

Normally, PITX2 mRNA displays a rapid turnover rate, but activation of the Wnt/β-catenin pathway stabilizes PITX2 mRNA (33). In fact, PITX2 is rapidly induced by the Wnt/Dvl/β-catenin pathway and is required for effective cell type–specific proliferation during pituitary development by directly activating cyclin D2 expression (34). Regulated exchange of HDAC1/β-catenin converts PITX2 from repressor to activator, analogous to the control of TCF/LEF1. PITX2 serves as a competence factor that is required for the temporally ordered and growth factor–dependent recruitment of a series of specific coactivator complexes that prove necessary for cyclin D2 and cyclin D1 (35) gene induction. Although we observed increased cyclin D1 levels, cyclin D2 expression was not increased. In addition, SFRP1 levels were up-regulated 9-fold, and SFRP1 has been shown to be capable of increasing Wnt signaling rather than antagonizing it in some conditions (36, 37). Taken together, the changes we observed in SFRP1, PITX2, and cyclin D1 are all consistent with a model in which elevated Wnt/β-catenin signaling is important for nonfunctional pituitary adenomas (Fig. 3). Moreover, increased nuclear accumulation of β-catenin has been detected by immunohistochemistry in 57% of pituitary adenomas (38), consistent with our conclusion that the Wnt/β-catenin pathway is important in the progression of this malignancy.

NOTCH3 is strongly overexpressed, whereas *DLK1*, a potential ligand of NOTCH3, was one of the most strongly down-regulated gene in nonfunctional tumors. Members of the delta family serve as ligands in cell-to-cell interactions with Notch receptors that control cell fate during differentiation. Interaction of Notch receptors with their cell-bound ligands results in the proteolytic cleavage of Notch, translocation of the intracellular domain (Notch-IC) to the nucleus, and altered gene expression. Emerging data also support the role of the Notch signaling pathway in tumorigenesis and neural development. Constitutive expression of NOTCH3-IC in the peripheral epithelium in the developing lung of transgenic mice resulted in altered lung morphology and delayed development, suggesting that NOTCH3 signaling could contribute to lung cancer

progression through the inhibition of terminal differentiation (39). Moreover, transgenic mice expressing NOTCH3-IC in thymocytes and T cells developed early and aggressive T-cell neoplasias (40). NOTCH3 and DLK1 expression is inversely correlated in neuroblastoma cell lines that can be divided into two groups with high DLK1/low NOTCH3 expression, or high NOTCH3/low DLK1 expression (41). Importantly, this study found a perfect correlation of mRNA and protein levels for both NOTCH3 and DLK1 (41). In neuroendocrine cell differentiation, changes in DLK1 levels seem to mark the decision to mature along different lineages. Thus, the high levels of NOTCH3 and low levels of DLK1 in nonfunctional pituitary adenomas suggest that they are derived from earlier-stage, undifferentiated cells, or that they have taken on a dedifferentiated state, consistent with the loss of Pit-1 expression.

The nonfunctional adenoma cells seem to have switched from a delta-expressing cell type to a Notch-expressing cell type and might receive stimulatory signals from neighboring normal pituitary cells that still express DLK1. This hypothesis suggests that inhibitors of Notch processing, such as γ-secretase inhibitors that were developed for Alzheimer's therapies and are now in clinical trials to treat Notch-activated T-cell acute lymphoblastic leukemia (42), could also prove of benefit to patients with nonfunctional pituitary adenomas.

Another gene involved in the delta-Notch pathway that was strongly down-regulated in nonfunctional adenomas was *ASCL1*. In *Drosophila*, Achaete-Scute genes are upstream of and directly activate the expression of delta and Notch (43), and in developing mouse neuroendocrine cells, DLK1 expression depends on the mouse Achaete-Scute homologue (44). Furthermore, high levels of Notch signaling can induce the transcriptional silencing of ASCL1 (45). Thus, the high levels of NOTCH3 could repress ASCL1 leading to the loss of DLK1 expression in nonfunctional adenomas. Transducin-like enhancer of split 2 (TLE2) is a mammalian homologue of the *Drosophila* transcriptional repressor *groucho*, which represses targets of β-catenin. TLE2 interacts with HES-1 and is expressed during neuronal development (46). Thus, TLE2, which was up-regulated 2-fold in nonfunctional adenomas, is a link between Wnt-signaling and Notch signaling. These data support a model (Fig. 3) in which NOTCH3 represses HASH1 and in cooperation with Wnt signaling; NOTCH3 maintains in these tumors in an undifferentiated state.

Acknowledgments

Received 3/16/2005; revised 8/3/2005; accepted 9/3/2005.

Grant support: Department of Neurosurgery (N.M. Oyesiku), NIH grants K22-CA96560 (C.S. Moreno) and R01-CA106826 (C.S. Moreno), NS 42843 (D.M. Desiderio), RR-10522 (D.M. Desiderio), RR-14593 (D.M. Desiderio), and NSF DBI 9604633 (D.M. Desiderio).

The costs of publication of this article were defrayed in part by the payment of page charges. This article must therefore be hereby marked *advertisement* in accordance with 18 U.S.C. Section 1734 solely to indicate this fact.

We thank the Department of Neuropathology, Emory University Hospital for the histology and immunohistochemistry analyses.

References

1. Greenman Y, Melmed S. Diagnosis and management of nonfunctioning pituitary tumors. Annu Rev Med 1996;47:95–106.
2. Asa SL, Ezzat S. The cytogenesis and pathogenesis of pituitary adenomas. Endocr Rev 1998;19:798–827.
3. Asa SL, Kovacs K. Clinically non-functioning human pituitary adenomas. Can J Neurol Sci 1992;19:228–35.
4. Black PM, Hsu DW, Klibanski A, et al. Hormone production in clinically nonfunctioning pituitary adenomas. J Neurosurg 1987;66:244–50.
5. Katznelson L, Alexander JM, Klibanski A. Clinical review 45: clinically nonfunctioning pituitary adenomas. J Clin Endocrinol Metab 1993;76:1089–94.
6. Herman V, Fagin J, Gonsky R, Kovacs K, Melmed S. Clonal origin of pituitary adenomas. J Clin Endocrinol Metab 1990;71:1427–33.
7. Alexander JM, Biller BM, Bikkal H, Zervas NT, Arnold A, Klibanski A. Clinically nonfunctioning pituitary tumors are monoclonal in origin. J Clin Invest 1990;86:336–40.
8. Evans CO, Brown MR, Parks JS, Oyesiku NM. Screening for MEN1 tumor suppressor gene mutations in sporadic pituitary tumors. J Endocrinol Invest 2000;23:304–9.
9. Satta MA, Korbonits M, Jacobs RA, et al. Expression of menin gene mRNA in pituitary tumours. Eur J Endocrinol 1999;140:358–61.
10. Farrell WE, Simpson DJ, Bicknell J, et al. Sequence analysis and transcript expression of the MEN1 gene in sporadic pituitary tumours. Br J Cancer 1999;80:44–50.
11. Shimon I, Melmed S. Genetic basis of endocrine disease: pituitary tumor pathogenesis. J Clin Endocrinol Metab 1997;82:1675–81.
12. Spada A, Faglia G. G-protein dysfunction in pituitary tumors. In: Melmed S., editor. Oncogenesis and molecular biology of pituitary tumors. Vol. 20. Basel: Karger; 1996. p. 108–21.
13. Gittoes NJ. Current perspectives on the pathogenesis of clinically non-functioning pituitary tumours. J Endocrinol 1998;157:177–86.
14. Chaidarun SS, Eggo MC, Sheppard MC, Stewart PM. Expression of epidermal growth factor (EGF), its receptor, and related oncoprotein (erbB-2) in human pituitary tumors and response to EGF *in vitro*. Endocrinology 1994;135:2012–21.
15. Evans CO, Reddy P, Brat DJ, et al. Differential expression of folate receptor in pituitary adenomas. Cancer Res 2003;63:4218–24.
16. Evans CO, Young AN, Brown MR, et al. Novel patterns of gene expression in pituitary adenomas identified by complementary deoxyribonucleic acid microarrays and quantitative reverse transcription-polymerase chain reaction. J Clin Endocrinol Metab 2001;86:3097–107.
17. Tusher VG, Tibshirani R, Chu G. Significance analysis of microarrays applied to the ionizing radiation response. Pro Natl Acad Sci U S A 2001;98:5116–21.
18. Zhan X, Desiderio DM. A reference map of a human pituitary adenoma proteome. Proteomics 2003;3:699–713.
19. Zhan X, Desiderio DM. Spot volume vs. amount of protein loaded onto a gel: a detailed, statistical comparison of two gel electrophoresis systems. Electrophoresis 2003;24:1818–33.
20. Zhan X, Desiderio DM. Differences in the spatial and quantitative reproducibility between two second-dimensional gel electrophoresis systems. Electrophoresis 2003;24:1834–46.
21. Zhan X, Desiderio DM. Heterogeneity analysis of the human pituitary proteome. Clin Chem 2003;49:1740–51.
22. Iavarone A, Lasorella A. Id proteins in neural cancer. Cancer Lett 2004;204:189–96.
23. Nakamura N, Ramaswamy S, Vazquez F, Signoretti S, Loda M, Sellers WR. Forkhead transcription factors are critical effectors of cell death and cell cycle arrest downstream of PTEN. Mol Cell Biol 2000;20:8969–82.
24. Haselbeck RJ, McAlister-Henn L. Function and expression of yeast mitochondrial NAD- and NADP-specific isocitrate dehydrogenases. J Biol Chem 1993;268:12116–22.
25. Jo SH, Son MK, Koh HJ, et al. Control of mitochondrial redox balance and cellular defense against oxidative damage by mitochondrial NADP$^+$-dependent isocitrate dehydrogenase. J Biol Chem 2001;276:16168–76.
26. Kim SY, Park JW. Cellular defense against singlet oxygen-induced oxidative damage by cytosolic NADP$^+$-dependent isocitrate dehydrogenase. Free Radic Res 2003;37:309–16.
27. Mazurek S, Grimm H, Oehmke M, Weisse G, Teigelkamp S, Eigenbrodt E. Tumor M2-PK and glutaminolytic enzymes in the metabolic shift of tumor cells. Anticancer Res 2000;20:5151–4.
28. Mazurek S, Weisse G, Wust G, Schafer-Schwebel A, Eigenbrodt E, Friis RR. Energy metabolism in the involuting mammary gland. In Vivo 1999;13:467–77.
29. Pellegrini-Bouiller I, Manrique C, Gunz G, et al. Expression of the members of the Ptx family of transcription factors in human pituitary adenomas. J Clin Endocrinol Metab 1999;84:2212–20.
30. Parks JS, Brown MR. Transcription factors regulating pituitary development. Growth Horm IGF Res 1999;9 Suppl B:2–8; discussion 8–11.
31. Szeto DP, Ryan AK, O'Connell SM, Rosenfeld MG. P-OTX: a PIT-1 interacting homeodomain factor expressed during anterior pituitary gland development. Proc Natl Acad Sci U S A 1996;93:7706–10.
32. Simmons DM, Voss JW, Ingraham HA, et al. Pituitary cell phenotypes involve cell-specific Pit-1 mRNA translation and synergistic interactions with other classes of transcription factors. Genes Dev 1990;4:695–711.
33. Briata P, Ilengo C, Corte G, et al. The Wnt/β-catenin–>Pitx2 pathway controls the turnover of Pitx2 and other unstable mRNAs. Mol Cell 2003;12:1201–11.
34. Kioussi C, Briata P, Baek, SH, et al. Identification of a Wnt/Dvl/β-catenin–>Pitx2 pathway mediating cell-type-specific proliferation during development. Cell 2002;111:673–85.
35. Baek SH, Kioussi C, Briata P, et al. Regulated subset of G_1 growth-control genes in response to derepression by the Wnt pathway. Proc Natl Acad Sci U S A 2003;100:3245–50.
36. Kawano Y, Kypta R. Secreted antagonists of the Wnt signalling pathway. J Cell Sci 2003;116:2627–34.
37. Uren A, Reichsman F, Anest V, et al. Secreted frizzled-related protein-1 binds directly to Wingless and is a biphasic modulator of Wnt signaling. J Biol Chem 2000;275:4374–82.
38. Semba S, Han SY, Ikeda H, Horii A. Frequent nuclear accumulation of β-catenin in pituitary adenoma. Cancer 2001;91:42–8.

39. Dang TP, Eichenberger S, Gonzalez A, Olson S, Carbone DP. Constitutive activation of Notch3 inhibits terminal epithelial differentiation in lungs of transgenic mice. Oncogene 2003;22:1988–97.
40. Bellavia D, Campese AF, Checquolo S, et al. Combined expression of pTα and Notch3 in T cell leukemia identifies the requirement of preTCR for leukemogenesis. Proc Natl Acad Sci U S A 2002;99:3788–93.
41. Van Limpt VA, Chan AJ, Van Sluis PG, Caron HN, Van Noesel CJ, Versteeg R. High delta-like 1 expression in a subset of neuroblastoma cell lines corresponds to a differentiated chromaffin cell type. Int J Cancer 2003;105:61–9.
42. Weng AP, Ferrando AA, Lee W, et al. Activating mutations of NOTCH1 in human T cell acute lymphoblastic leukemia. Science 2004;306:269–71.
43. Heitzler P, Bourouis M, Ruel L, Carteret C, Simpson P. Genes of the Enhancer of split and achaete-scute complexes are required for a regulatory loop between Notch and Delta during lateral signaling in *Drosophila*. Development 1996;122:161–71.
44. Ito T, Udaka N, Yazawa T, et al. Basic helix-loop-helix transcription factors regulate the neuroendocrine differentiation of fetal mouse pulmonary epithelium. Development 2000;127:3913–21.
45. Ball DW. Achaete-scute homolog-1 and Notch in lung neuroendocrine development and cancer. Cancer Lett 2004;204:159–69.
46. Grbavec D, Lo R, Liu Y, Stifani S. Transducin-like Enhancer of split 2, a mammalian homologue of *Drosophila* Groucho, act as a transcriptional repressor, interacts with Hairy/Enhancer of split proteins, and is expressed during neuronal development. Eur J Biochem 1998;258:339–49.

Novel Molecular Signaling and Classification of Human Clinically Nonfunctional Pituitary Adenomas Identified by Gene Expression Profiling and Proteomic Analyses

Carlos S. Moreno, Chheng-Orn Evans, Xianquan Zhan, et al.

Cancer Res 2005;65:10214-10222.